Electronic Supplementary Material (ESI) for Journal of Materials Chemistry A.

Pine Cone Shell Based Activated Carbon Used for CO_2 Adsorption

Kaimin Li, [a] *Sicong Tian,* [a] *Jianguo Jiang,* *, [a, b, c] *Jiaming Wang,* [a] *Xuejing Chen,* [a] *Feng Yan* [a]

[a] School of Environment, Tsinghua University, Beijing 100084, China

[b] Key Laboratory for Solid Waste Management and Environment Safety, Ministry of Education of China, China

[c] Collaborative Innovation Center for Regional Environmental Quality, Tsinghua University, Beijing 100084, China

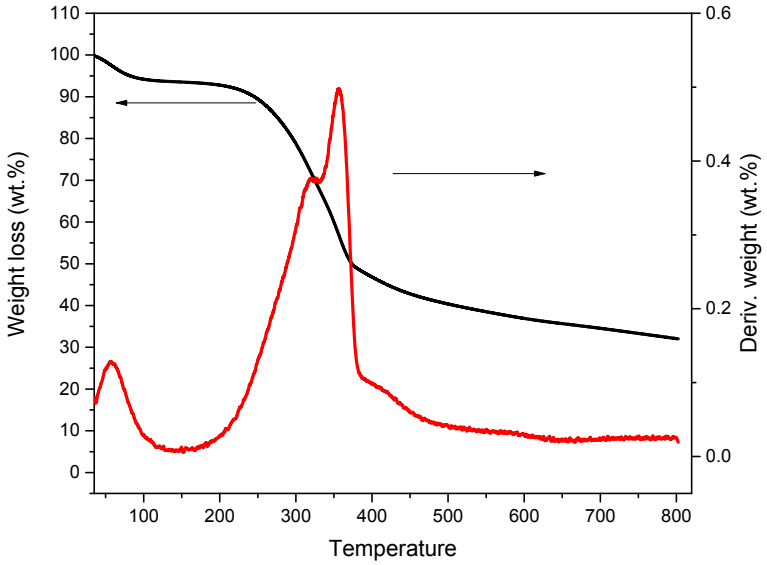

Fig. S1 Temperature programming test for pine cone shells with a thermogravimetric analyzer (Mettler Toledo TGA/DSC 2 thermogravimetric analyzer) was conducted under N_2 of 60ml/min from 35°C to 800°C with a heating rate of 5°C/min. Results show that two obvious weight loss stages occurred in the process: when the temperature is lower than 100°C the weight loss was mainly due to the loss of physisorption water; and from 200°C to 400°C the weight loss was mainly due to the pyrolysis of pine cone shells, the differential curves of weight to temperature also supports this conclusion. After 400°C, the loss rate of weight became slow, however a weak peak also appeared in the differential curve of weight to temperature between 400°C to 500°C, and a weight loss of 6.2% also occurred for 400°C to 500°C, therefore, 500°C was chose as the carbonation temperature to produce stable activated carbon materials.

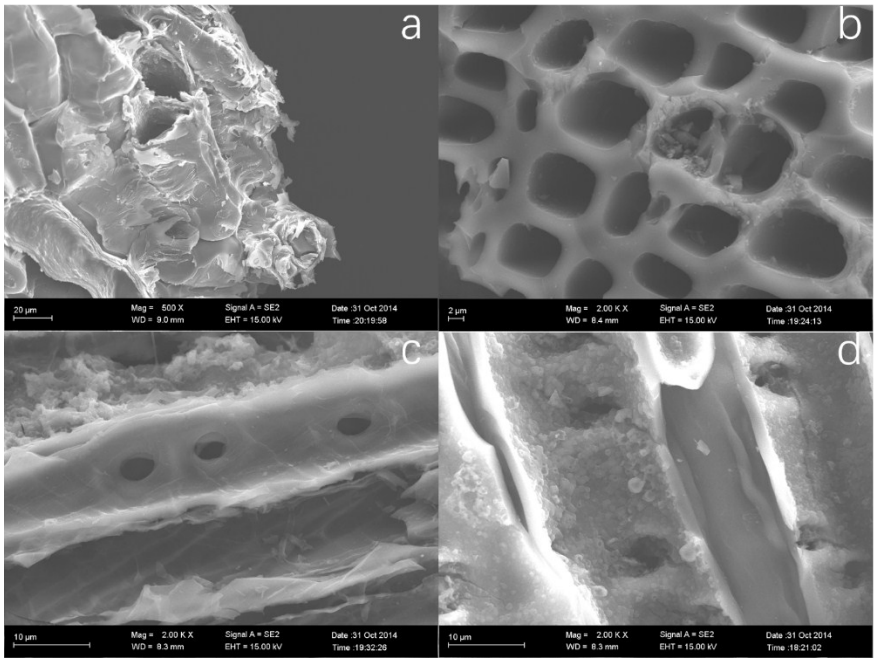

Fig. S2 SEM images: (a) for pine cone shell; (b) and (c) for Non-PAC; (d) for PAC-650/2.

Table S1. The elemental C, O, N, and H content for all activated carbons and yield of pine cone shells-based activated carbons under different preparation conditions.

Sample	Elemental content (wt.%)				Yield (wt.%) [a]
	C	O	N	H	
Pine cone shell	46.62	38.63	1.33	5.09	NA [b]
Non-PAC	75.84	12.12	1.29	2.99	42
PAC-500/2	68.17	22.12	0.84	2.72	38
PAC-550/2	71.67	19.60	0.90	2.28	37
PAC-600/2	80.50	12.13	0.79	1.43	35
PAC-650/2	85.08	9.26	1.03	1.07	35
PAC-700/2	88.39	7.94	0.52	0.74	34
PAC-750/2	91.79	5.29	0.45	0.49	23
PAC-800/2	93.28	4.48	0.65	0.41	12
PAC-500/1	72.61	17.13	1.09	2.76	37
PAC-500/3	69.57	20.73	0.72	2.24	38
PAC-500/4	69.72	22.21	0.63	2.11	38

[a] the yield is determined according to 1 g pine cone shell. [b] NA means not available.

Table S2 The comparison between the PAC-500/1 and other activated carbons in adsorption capacity at 298 K and 0.15 bar, and adsorption selectivity of CO_2 to N_2 at 298 K.

Sample	CO_2 adsorption capacity	Adsorption selectivity of CO_2	Increasing proportions in	Decreasing proportions in

	(mmol/g)	to N_2	CO_2 adsorption capacity (%)	adsorption selectivity (%)
PAC-650/2	1.2	17	0.12	0.62
PAC-550/2	1.14	26	0.065	0.42
PAC-600/2	1.12	18	0.047	0.6
PAC-500/2	1.11	36	0.037	0.2
PAC-500/1	1.07	45	0	0

Table S3 The CO_2 adsorption capacity of activated carbons under 0.15 bar and 1 bar at 273 K, 298 K, and 318 K, and the N_2 adsorption capacity of activated carbons under 0.85 bar and 1bar at 298 K, and the adsorption selectivity of CO_2 to N_2 at 298 K.

sample	CO_2 adsorption capacity (mmol/g)						N_2 adsorption capacity (mmol/g)		Adsorption selectivity of CO_2 to N_2
	0°C		25°C		45°C		25°C		
	0.15bar	1bar	0.15bar	1bar	0.15bar	1bar	0.85bar	1bar	
N-PAC	1.12	2.19	0.62	1.55	0.37	1.11	0.11	0.13	76
PAC-500/2	2.06	4.79	1.11	3.23	0.60	2.16	0.28	0.32	36
PAC-550/2	2.27	6.05	1.14	3.83	0.65	2.58	0.34	0.39	26
PAC-600/2	2.32	6.97	1.12	4.17	0.67	2.87	0.43	0.50	18
PAC-650/2	2.35	7.63	1.20	4.73	0.65	2.98	0.49	0.56	17
PAC-700/2	2.16	7.67	1.02	4.34	0.59	2.85	0.50	0.57	13
PAC-750/2	2.01	7.30	0.97	4.22	0.56	2.72	0.50	0.57	13
PAC-800/2	1.81	7.10	0.92	4.13	0.55	2.71	0.49	0.56	12
PAC-500/1	1.97	3.93	1.07	2.79	0.65	2.01	0.25	0.29	45
PAC-500/3	1.58	3.83	0.85	2.52	0.50	1.73	0.21	0.24	37
PAC-500/4	1.56	3.94	0.84	2.57	0.47	1.76	0.21	0.25	35

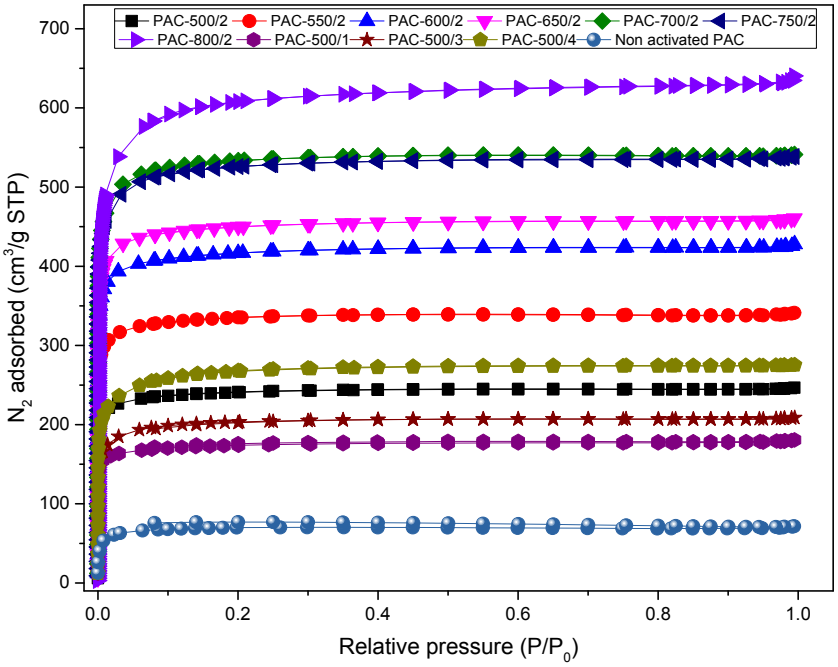

Fig. S3 N_2 adsorption-desorption results for all activated carbon products.

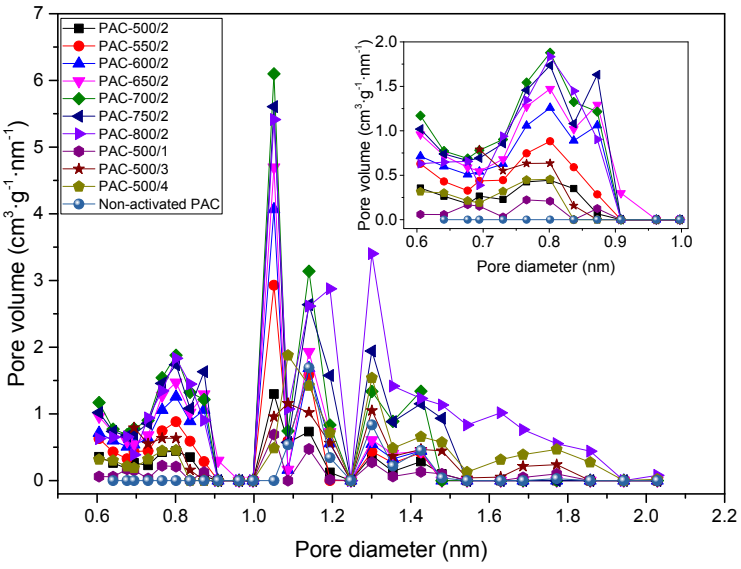

Fig. S4 Pore size distribution for all activated carbons calculated using the N_2 adsorption data with the NLDFT method.

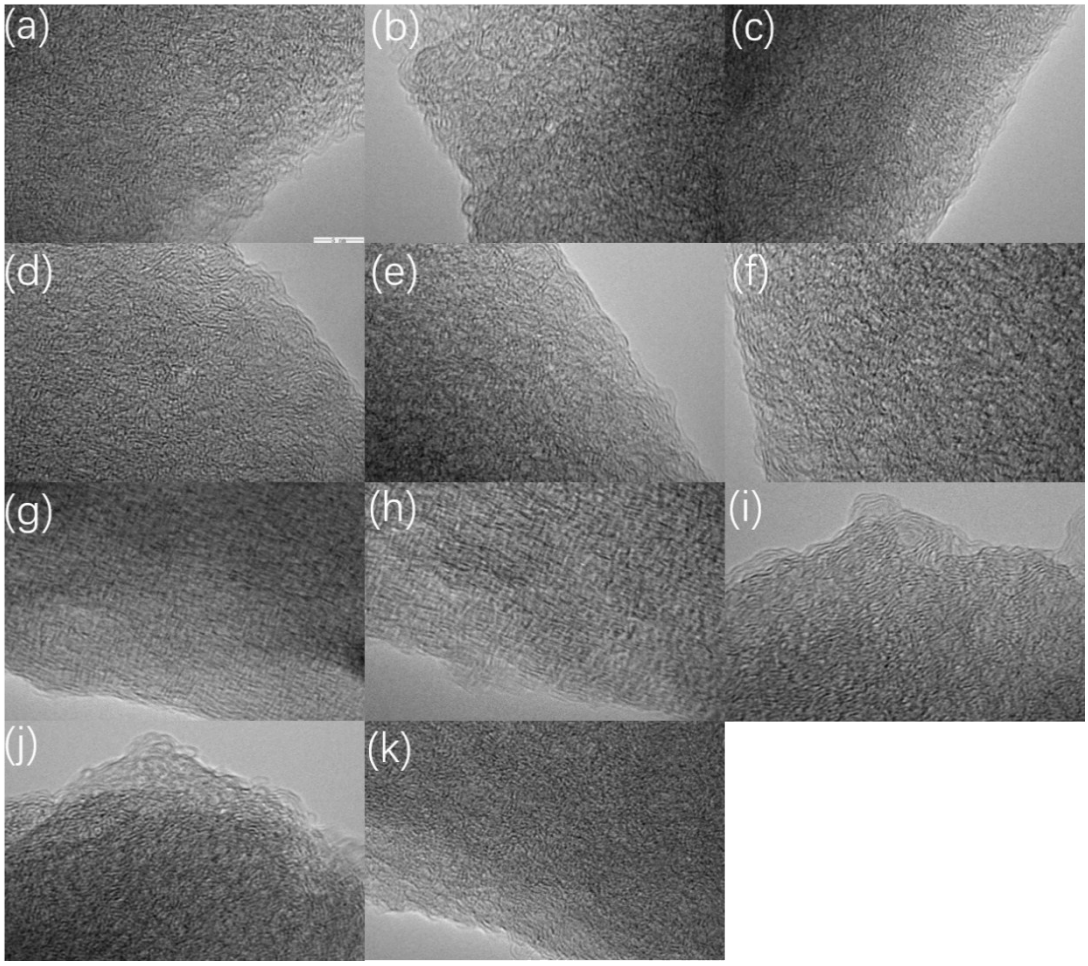

Fig. S5 TEM images (magnified 1.5 million times) for all activated carbons: (a) for Non-PAC; (b) for PAC-500/2; (c) for PAC-550/2; (d) for PAC-600/2; (e) for PAC-650/2; (f) for PAC-700/2; (g) for PAC-750/2; (h) for PAC-800/2; (i) for PAC-500/1; (j) for PAC-500/3; (k) for PAC-500/4.

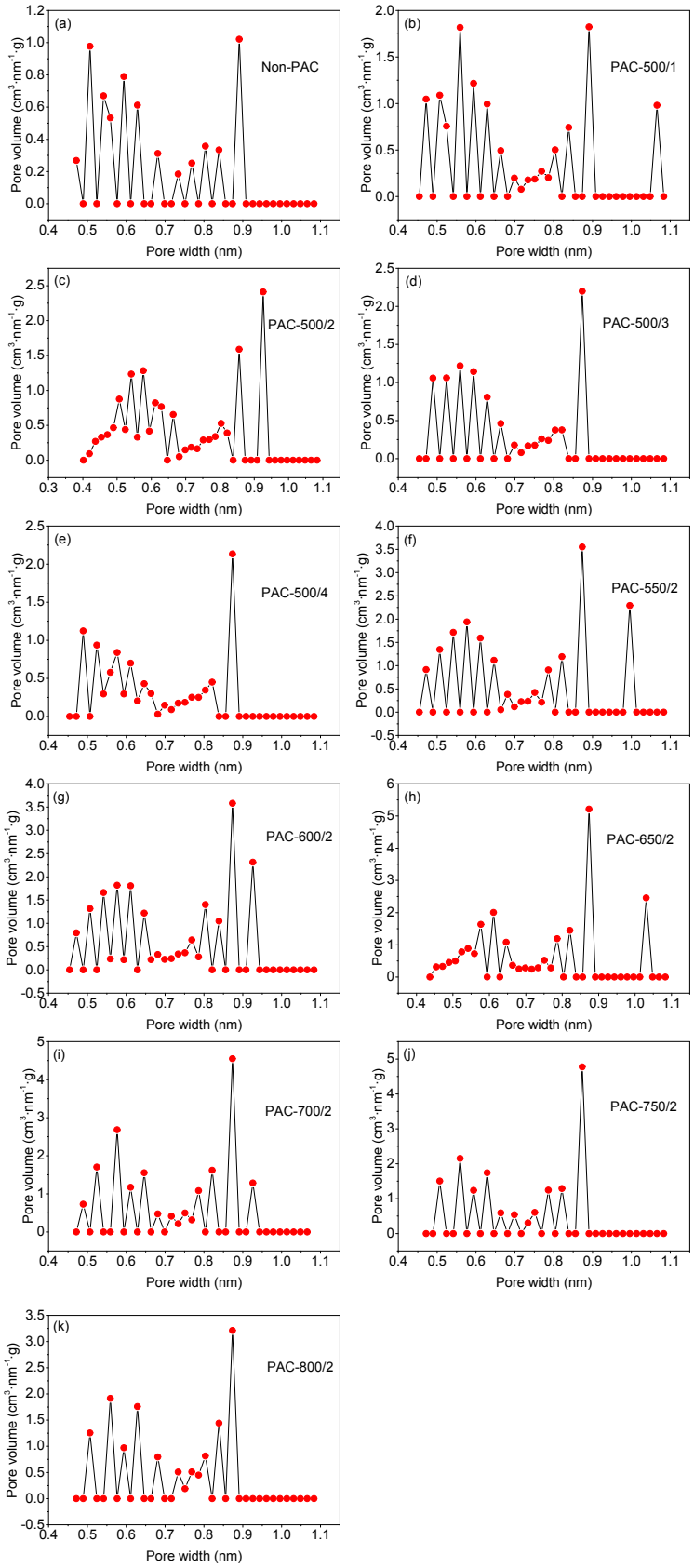

Fig. S6 The micropore distribution of activated carbons calculated with CO_2 adsorption results at 273 K: (a) Non-PAC; (b) PAC-500/1; (c) PAC-500/2; (b) PAC-500/3; (b) PAC-500/4; (b) PAC-

550/2; (b) PAC-600/2; (b) PAC-650/2; (b) PAC-700/2; (b) PAC-750/2; (b) PAC-800/2.

Table S4 BET surface area and total pore volume of activated carbons.

Sample	BET surface area (m^2/g)	Total pore volume (cm^3/g) [a]
Non-PAC	589	0.11
PAC-500/2	1486	0.38
PAC-550/2	2122	0.53
PAC-600/2	2526	0.66
PAC-650/2	3135	0.71
PAC-700/2	3529	0.84
PAC-750/2	3759	0.83
PAC-800/2	3931	0.99
PAC-500/1	1246	0.28
PAC-500/3	1402	0.32
PAC-500/4	1772	0.43

[a] calculated from the N_2 adsorption results at the relative pressure (P/P_0) is 0.99.

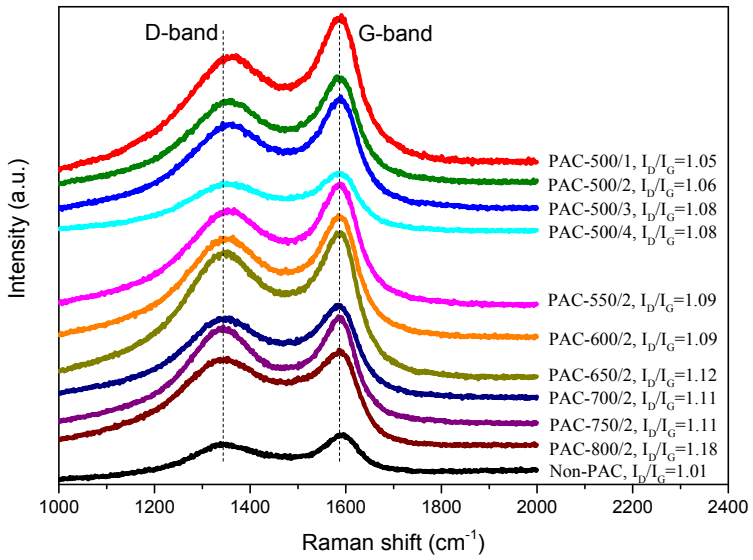

Fig. S7 The Raman spectrum of activated carbons collected using a Renishaw inVia laser Raman spectrometer (UK) with a 532 nm laser source.

Table S5 The single-site Langmuir model (equation (S1)) or dual-site Langmuir model (equation (S2)) is used to fit CO_2 adsorption isotherms of activated carbons and the fitting results are shown in Fig. S1 to S11:

$$q = \frac{q_{sat} bp}{1 + bp} \qquad (S1)$$

$$q \equiv q_A + q_B = \frac{q_{sat,A} b_A p}{1 + b_A p} + \frac{q_{sat,B} b_B p}{1 + b_B p} \qquad (S2)$$

where q is amount of CO_2 adsorbed (mmol/g), q_{sat} is saturation adsorption capacity (mmol/g), and b is equilibrium constant (Pa^{-1}).

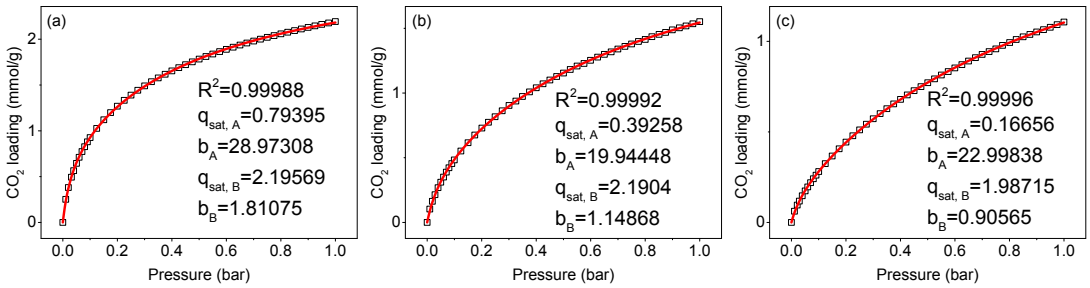

Fig. S8 The dual-site Langmuir fitting for CO_2 adsorption isotherms of Non-PAC: (a) at 273 K; (b) at 298 K; (c) at 318 K, (□) is the experimental data and the red line (-) is the fitting results.

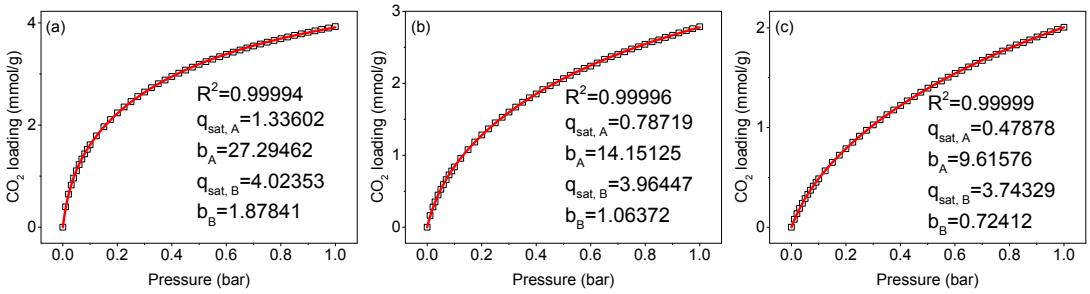

Fig. S9 The dual-site Langmuir fitting for CO_2 adsorption isotherms of PAC-500/1: (a) at 273 K; (b) at 298 K; (c) at 318 K, square (□) is the experimental data and the red line (-) is the fitting results.

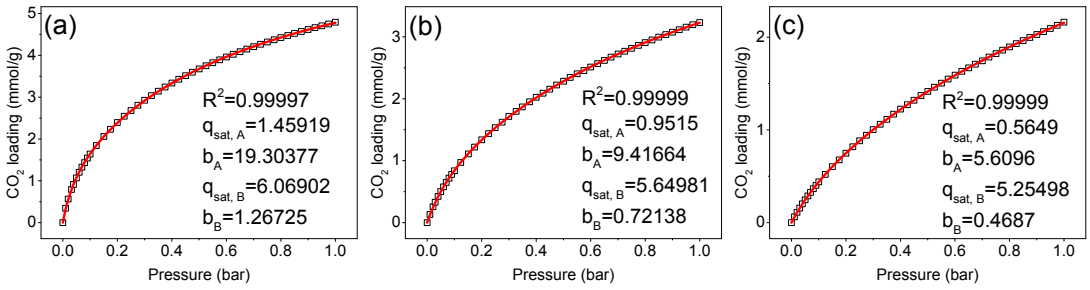

Fig. S10 The dual-site Langmuir fitting for CO_2 adsorption isotherms of PAC-500/2: (a) at 273 K; (b) at 298 K; (c) at 318 K, square (□) is the experimental data and the red line (-) is the fitting results.

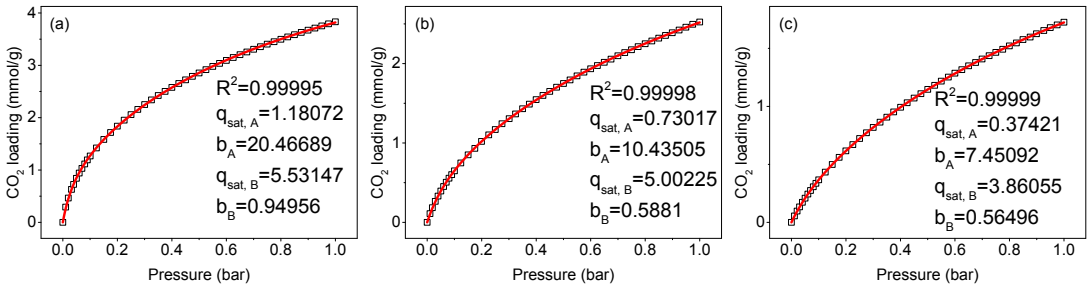

Fig. S11 The dual-site Langmuir fitting for CO_2 adsorption isotherms of PAC-500/3: (a) at 273 K; (b) at 298 K; (c) at 318 K, square (□) is the experimental data and the red line (-) is the fitting results.

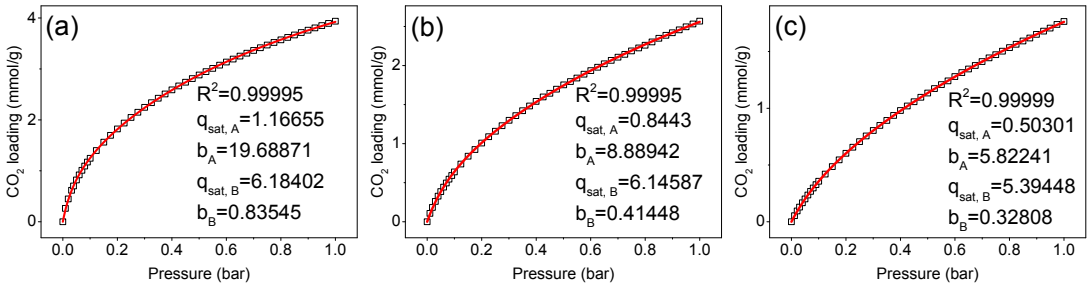

Fig. S12 The dual-site Langmuir fitting for CO_2 adsorption isotherms of PAC-500/4: (a) at 273 K; (b) at 298 K; (c) at 318 K, square (□) is the experimental data and the red line (-) is the fitting results.

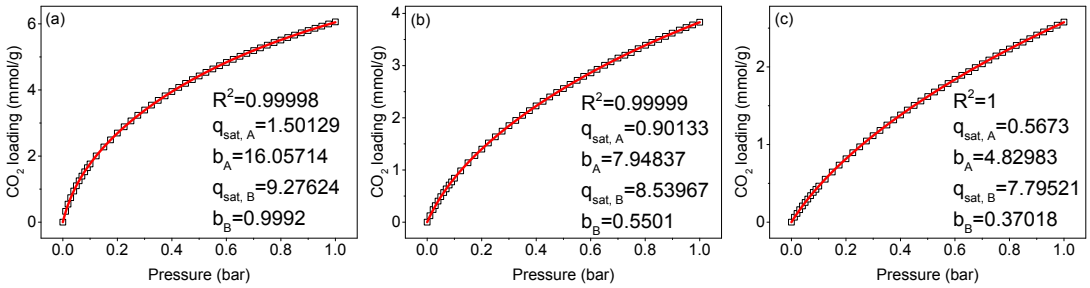

Fig. S13 The dual-site Langmuir fitting for CO_2 adsorption isotherms of PAC-550/2: (a) at 273 K; (b) at 298 K; (c) at 318 K, square (□) is the experimental data and the red line (-) is the fitting results.

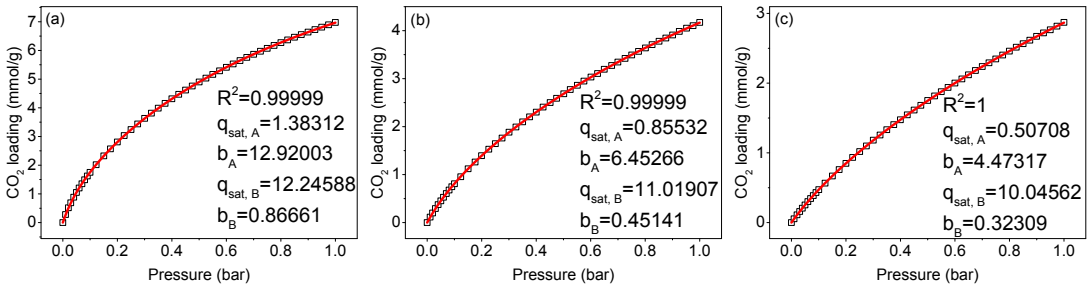

Fig. S14 The dual-site Langmuir fitting for CO_2 adsorption isotherms of PAC-600/2: (a) at 273 K; (b) at 298 K; (c) at 318 K, square (□) is the experimental data and the red line (-) is the fitting results.

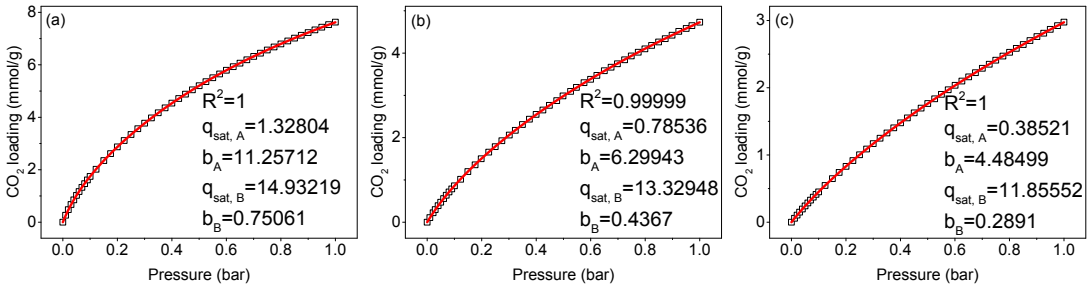

Fig. S15 The dual-site Langmuir fitting for CO_2 adsorption isotherms of PAC-650/2: (a) at 273 K; (b) at 298 K; (c) at 318 K, square (□) is the experimental data and the red line (-) is the fitting results.

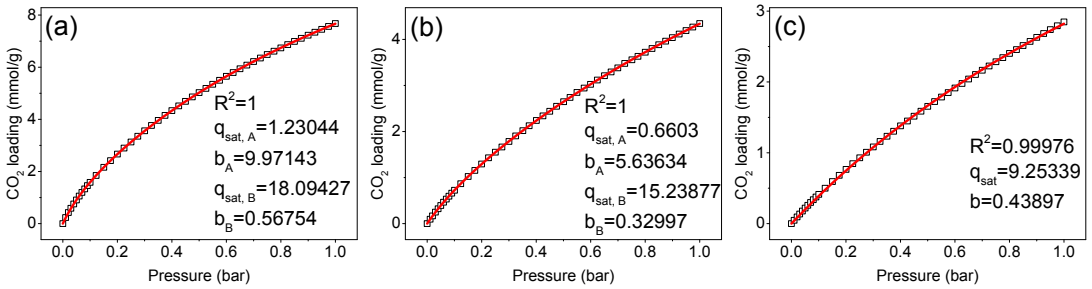

Fig. S16 The dual-site Langmuir fitting for CO_2 adsorption isotherms of PAC-700/2: (a) at 273 K; (b) at 298 K; and single-site Langmuir fitting for CO_2 adsorption isotherms of PAC-700/2: (c) at 318 K (under this condition the single-site Langmuir model can achieve a better fitting result than dual-site Langmuir model), square (□) is the experimental data and the red line (-) is the fitting results.

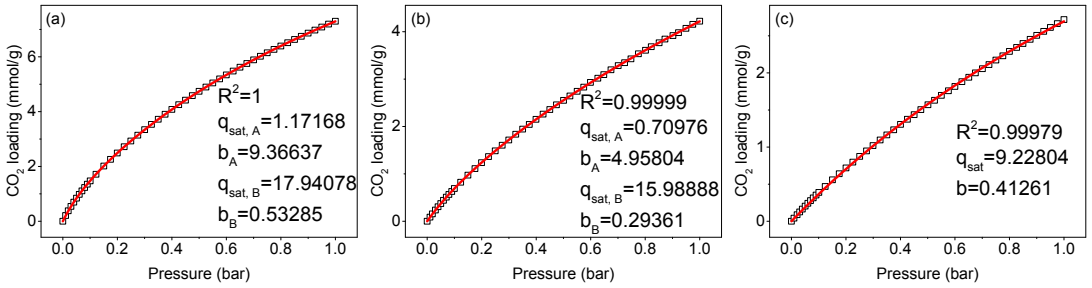

Fig. S17 The dual-site Langmuir fitting for CO_2 adsorption isotherms of PAC-750/2: (a) at 273 K; (b) at 298 K; and single-site Langmuir fitting for CO_2 adsorption isotherms of PAC-750/2: (c) at 318 K (under this condition the single-site Langmuir model can achieve a better fitting result than dual-site Langmuir model), square (□) is the experimental data and the red line (-) is the fitting results.

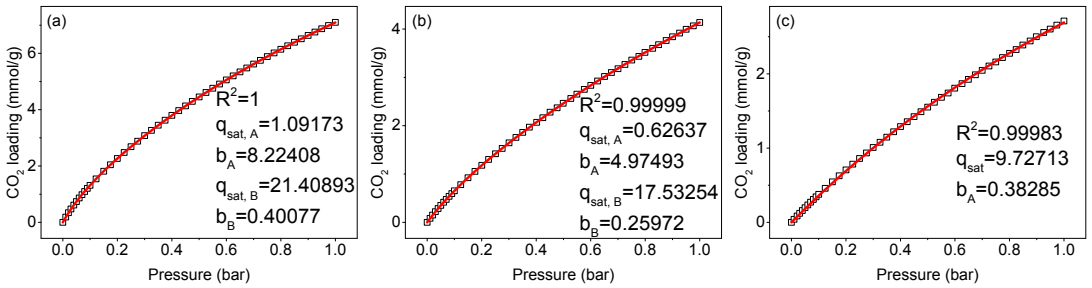

Fig. S18 The dual-site Langmuir fitting for CO_2 adsorption isotherms of PAC-800/2: (a) at 273 K; (b) at 298 K; and single-site Langmuir fitting for CO_2 adsorption isotherms of PAC-800/2: (c) at 318 K (under this condition the single-site Langmuir model can achieve a better fitting result than dual-site Langmuir model), square (□) is the experimental data and the red line (-) is the fitting results.

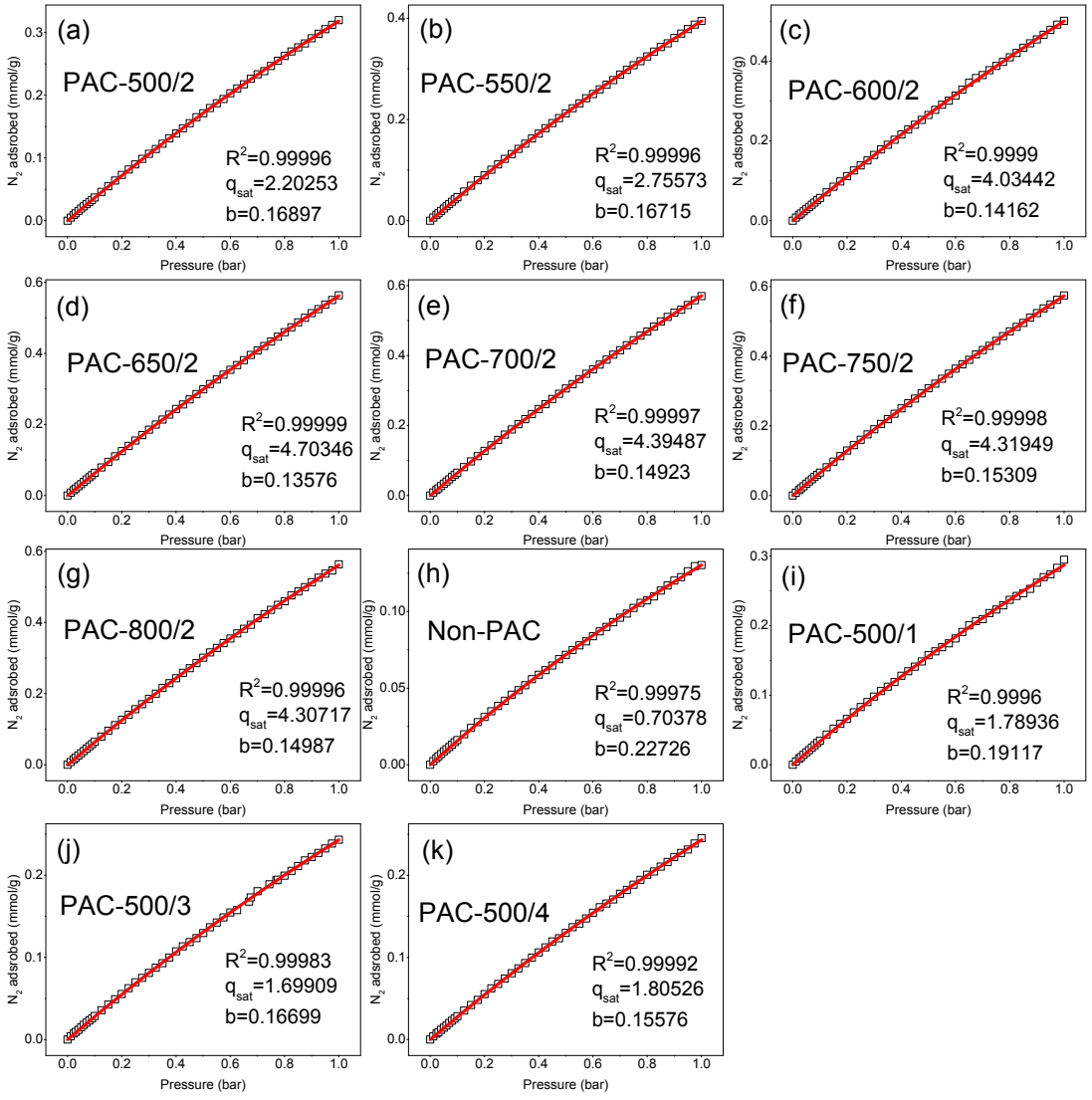

Fig. S19 The single-site Langmuir model fitting results for N_2 adsorption isotherms of activated carbons at 298 K: (a) for PAC-500/2; (b) for PAC-550/2; (c) for PAC-600/2; (d) for PAC-650/2;

(e) for PAC-700/2; (f) for PAC-750/2; (g) for PAC-800/2; (h) for Non-PAC; (i) for PAC-500/1; (a) for PAC-500/3; (a) for PAC-500/4.

Table S6 The isosteric heat of CO_2 adsorption (Q_{st}) is calculated with Clausius-Clapeyron equation:

$$Q_{st} = RT^2\left(\frac{\partial lnP}{\partial T}\right)_\theta \qquad (S3)$$

where T is temperature (K), P is pressure (Pa), θ is coverage degree and R is gas constant (8.314 $J \cdot mol^{-1} \cdot K^{-1}$).

Equation (S2) can be expressed as:

$$lnP = -\frac{Q_{st}}{R} \times \frac{1}{T} + C \qquad (S4)$$

here C is a constant. Through building the linear fitting between T^{-1} and lnP, the Q_{st} can be obtained.

Table S7 The initial isosteric heat of CO_2 adsorption of activated carbons.

Sample	Initial isosteric heat of adsorption (kJ/mol)
Non-PAC	32.7
PAC-500/2	31.6
PAC-550/2	29.8
PAC-600/2	27.6
PAC-650/2	27.2
PAC-700/2	26.6
PAC-750/2	26.3
PAC-800/2	24.3
PAC-500/1	32.9
PAC-500/3	29.8
PAC-500/4	29.5

Table S8 Initial isosteric heat of CO_2 adsorption is the adsorption heat when the pressure P tends to zero, under very low pressure the adsorption isotherm can be depicted by Henry rule:

$$q = k \times P$$

where q is the amount of CO_2 adsorbed, p is the pressure and k is Henry factor.

Through building the linear correlation between P and ln(P/q), the absolute value of the intersection equals to the value of k, and the initial isosteric heat of CO_2 adsorption (Q_{st}^0) can be calculated with the following equation:

$$Q_{st}^0 = RT + R \times \frac{dk}{d(\frac{1}{T})}$$